Cluster model DFT study of the intermediates of benzene to phenol oxidation by N_2O on FeZSM-5 zeolites

Nelly A. Kachurovskaya [a,*], Georgii M. Zhidomirov [b], Emiel J.M. Hensen [a], and Rutger A. van Santen [a]

[a] *Schuit Institute of Catalysis, Laboratory of Inorganic Chemistry and Catalysis, Eindhoven University of Technology, PO Box 513, 5600MB, Eindhoven, The Netherlands*

[b] *Boreskov Institute of Catalysis, Pr. Lavrentieva 5, Novosibirsk 630090, Russia*

Received 13 August 2002; accepted 7 November 2002

An Fe(II) ion at an α-cation exchange position of ZSM-5 zeolite (Fe/Z) was taken as a model for the active site in the nitrous oxide decomposition and in the selective oxidation of phenol with nitrous oxide. The oxygen deposited by decomposition of N_2O is commonly referred to as α-oxygen (OFe/Z). Cluster model DFT calculations show that the interaction of the OFe/Z center with benzene resulted easily in arene oxide formation. The results indicate a rather low activation energy for this step. Possible transformations of the adsorbed arene oxide are considered and the experimental evidence for the absence of the kinetic H/D isotope effect in phenol formation is discussed. It is concluded that the rate-limiting step for the *in situ* oxidation of benzene to phenol is the desorption of the product.

KEY WORDS: phenol oxidation; zeolite; cluster calculations.

1. Introduction

Recently, the selective oxidation of hydrocarbons over ZSM-5 zeolite has attracted considerable attention. More specifically, the direct conversion of benzene to phenol over FeZSM-5 appears to present a potential alternative to the existing three-step cumene process. Despite intensive research there remain a large number of questions on the nature of the active sites and the catalytic mechanism of nitrous oxide decomposition and benzene oxidation. Studies have shown that the extra-framework Fe ions play a pivotal role [1–5]. The active Fe sites are commonly referred to as α-sites and their characteristic property is the adsorption of an oxygen atom upon decomposition of nitrous oxide. This α-oxygen atom is capable of selectively oxidizing benzene. At the same time it should be noted that the presence of Al or Ga in the lattice and of Brønsted acidity strongly promotes the formation of α-sites [6,7]. The structure of these active sites, however, has remained elusive.

In high-silica zeolites, Fe extra-framework species include (i) mononuclear cationic species, (ii) oxo-ions, which contain more than one iron ion cation bounded through extra-lattice oxygen, the most typical example being the binuclear oxo-bridged complex, and (iii) small extra-lattice iron oxide–hydroxide clusters [8]. Additionally, large agglomerates of iron oxide may be present on the external zeolite surface. The relative fraction of the several species strongly depends on the introduction method of the iron and the pretreatment procedure. Introduction of iron at the stage of zeolite synthesis provides a dispersed catalyst. Activation is performed by removing part of the iron from the framework [9,10] using high-temperature treatments, preferably steaming [11,12]. On the other hand, sublimation of $FeCl_3$ is a way to implant directly extra-framework Fe species in the zeolite micropore space. Such catalysts are active in nitrous oxide decomposition [13]. It has been proposed that binuclear clusters are the active species in this reaction [14,15] supported by EXAFS studies [16,17]. A realistic model of a binuclear complex, stabilized in two neighboring 5T rings, has been used in a theoretical study of nitrous oxide decomposition [18]. Here, we note that the pre-eminent formation of binuclear oxo-bridged complexes during sublimation is rather sensitive to the experimental conditions [16,17]. Zhu *et al.* [19] noted that calcination or steaming at 700 °C increases the nitrous oxide decomposition rate of sublimed Fe/ZSM-5.

Recent speculations point to the importance of Fe^{2+} an active species for the deposition of α-oxygen from nitrous oxide [20]. This is a correlation between the number of α-oxygen sites and the amount of reduced Fe^{2+} [9,20]. The specific nature of these sites is a matter of strong debate, especially regarding their nuclearity [2]. One proposal is that it concerns monoatomic species in a paired arrangement, which are detected as binuclear clusters by Mössbauer spectroscopy [9]. Since each of the iron ions is able to generate an α-oxygen atom, a model of the active site might be one Fe^{2+} cation. Besides, we also took into account the experimental evidence for the stabilization of isolated iron cations after steaming

* To whom correspondence should be addressed.
E-mail: N.A.Kachurovskaya@tue.nl

1011-372X/03/0300-0025/0

[19,21]. The siting of divalent ions has been studied both experimentally [22] and theoretically [23,24]. Ions exhibit preferences for the individual cationic sites α, β and γ [22]. The α-cation-exchange position of ZSM-5 is easily accessible for reactants in MFI. Unfortunately, there are only limited experimental data on the nature of α-oxygen and on the reaction intermediates. The bond energy of the oxygen atom in the α-oxygen structure was estimated to be about 250.8 kJ/mol [25]. Importantly the kinetic H/D isotope effect (KIE) in benzene oxidation by "α-oxygen" was found to be absent [26]. An intriguing vibrational frequency band at 2874 cm^{-1} was observed during the adsorption of benzene in a zeolite where α-oxygen was deposited. This band disappeared after evacuation at elevated temperature [27].

An earlier theoretical study of the reaction path for benzene oxidation [28] employed a 3T cluster. A direct insertion of oxygen into the C–H bond of benzene was considered. However, the choice of Fe^{1+} as the model for the α-site seems to be rather questionable. We consider another model and another reaction path.

2. Computational details

Density functional theory (DFT) calculations were carried out using the GAUSSIAN-98 program. The B3LYP hybrid functional [29] was employed. As indicated by Loh *et al.* [30], the B3LYP method correctly reproduces the experimental dissociation energy of FeO^+ (340.3 ± 5.9 kJ/mol). Glukhovtsev *et al.* [31] found upon examination of calculated geometries, bond dissociation energies, ionization energies, enthalpies of formation, and harmonic frequencies and their comparison with experimental and higher level (CCSD(T), MCPF, CASSCF) computations that B3LYP calculations of iron-containing species are capable of giving reliable results. A 6-31 G* basis set was used for all types of atoms. Our iron-containing models were calculated with four unpaired electrons because Fe(II) particles are paramagnetic. This configuration corresponds to the state with total spin 2. Computed $\langle S^2 \rangle$ values confirmed that the spin contamination included in calculations was very small.

We selected crystallographic data for the α-position of MFI as the initial model for cluster calculations (figure 1). This site is constructed from two intersecting five-membered zeolite rings, which forms a six-membered ring. In this ring two distant Si atoms were replaced by Al. Hydrogen atoms were used to saturate broken Si–O bonds. Usually, in cluster calculations hydrogen atoms are used to saturate the broken Al–O bond. However, this approximation introduces a significant error due to the difference in cationic radius between Si^{4+} and Al^{3+}. In our cluster Al atoms were saturated by $-OSiH_3$ groups. This allowed our model to be more flexible on replacing Si by Al. First, the positions of the boundary atoms were optimized with a frozen core and with saving the crystal structure directions of the boundary bonds. This optimization was carried out for the cluster with effective charge −2. All the following calculations were performed with full optimization of the inner region of the cluster and with fixed positions of hydrogen boundary atoms.

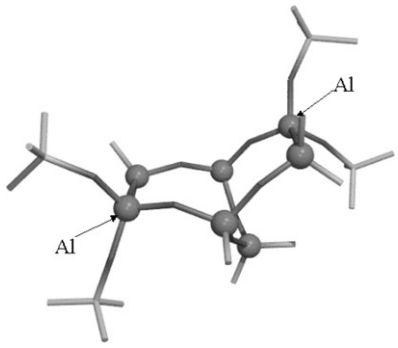

Figure 1. Initial model for cluster calculations (crystallographic α-position).

It is important to mention that we performed comparative calculations for the benzene to phenol transformation for three different cases: (i) on our cluster model of Fe/ZSM-5, (ii) on a cluster model only containing a Brønsted acid site and (iii) the uncatalyzed reaction in the gas phase. In the last case, a biradical was formed as the key intermediate. This structure is an open shell singlet system in which two electrons are located on two molecular orbitals. To calculate this system we used the complete active space multi-configuration SCF theory (CAS SCF) [32,33]. The chosen active space consists of two molecular orbitals with two electrons. Protonated benzene oxide and intermediate were treated as charged systems.

For the search of transition states the QST2 procedure was used. We also report the vibration frequencies of possible intermediates at the B3LYP/6-31G* level by evaluating analytically the second derivatives of energy with respect to the nuclear coordinates.

3. Results and discussion

The results will be discussed in three subsections. In the first, we will discuss the results of our search for the proper chemical model for α-oxygen deposited on iron. In the second, the reaction of this oxygen atom with benzene will be discussed. It should be emphasized that due to the model character of the present approach, we can only delineate a plausible set of intermediates having facile interconversions. In the final subsection, the rate-limiting step is considered for gas-phase molecules and for the case of an acid-catalyzed reaction.

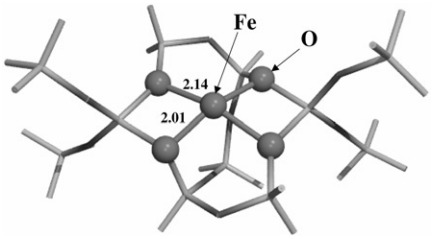

Figure 2. Optimized structure of Fe^{2+} in α-cationic exchange position.

3.1. Model for the "α-center"

Figure 2 shows the optimized structure of the Fe^{2+} ion, which represents our model for the α-site. The cation is stabilized by interaction with four oxygen ions of the effective six-membered ring of the α-cationic position. These four oxygens are from Si–O–Al fragments and the construction has a slightly pyramidal structure. The Fe–O bond distances are 2.01 and 2.14 Å. The spin density on the Fe ion equals 3.785, while the total atomic charge on iron is +0.672 corresponding to a Fe^{2+} oxidation state.

The next step is to generate the α-oxygen species responsible for the catalytic activity. The structure of such species is displayed in figure 3. This center is formed due to the decomposition of a nitrous oxide molecule on the α-site. The reaction energy associated with the reaction

$$Fe/Z + N_2O \rightarrow OFe/Z + N_2$$

is about −41.8 kJ/mol. The resulting Fe=O bond distance equals 1.59 Å corresponding to the bond distance in ferryl oxygen species. Charges on Fe and O ions are +0.937 and −0.314, respectively, and the total atomic spin densities on Fe and O are 3.406 and 0.329. This means that approximately all four unpaired electrons are located on the Fe cation. The Fe=O bond energy was calculated by evaluating the reaction energy for

$$2OFe/Z \Rightarrow 2Fe/Z + O_2$$

It equals 232.0 kJ/mol, which is in good agreement with the value of 250.8 ± 41.8 kJ/mol [25].

3.2. The reaction path for hydroxylation

Panov and co-workers [25] proposed that the reaction of benzene oxidation proceeds via the initial formation of unstable arene oxides, which can spontaneously isomerize into a phenolic product:

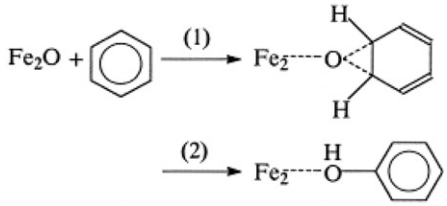

The experimental observation of a kinetic H/D isotope effect close to unity [26] led to the proposal of step (1) being rate limiting. The stability of arene oxides was studied in a number of works [34–36]. It was found that benzene arene oxide has two valence tautomers: benzene oxide and oxepin. The benzene oxide ↔ oxepin equilibrium is shifted toward oxepin in the gas phase. Our gas-phase calculations indeed show that oxepin is more stable by 2.9 kJ/mol than benzene oxide. This is in good agreement with the experimental value of 7.1 kJ/mol determined by ^{1}H NMR [37]. The transition state for the isomerization of benzene oxide to oxepin was calculated. The optimized structures are shown in figure 4, while values for the changes in total energies are collected in table 1. Vogel and Günther [38] experimentally determined the enthalpy of activation for isomerization of benzene oxide to oxepin to be 36.8 kJ/mol. We estimate the energy of activation to be 25.9 kJ/mol for the same reaction.

To study the catalytic mechanism, we tried to find an adsorption complex of the benzene molecule with our model cluster, OFe/Z. Depending on the initial geometry, either benzene oxide was formed or no adsorption of benzene took place. This points to a low activation

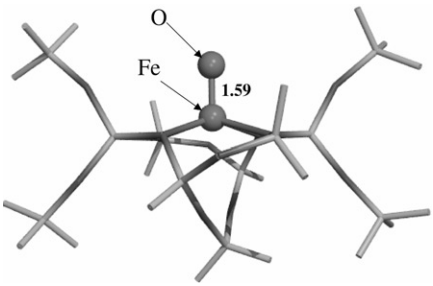

Figure 3. Structure of α-oxygen species.

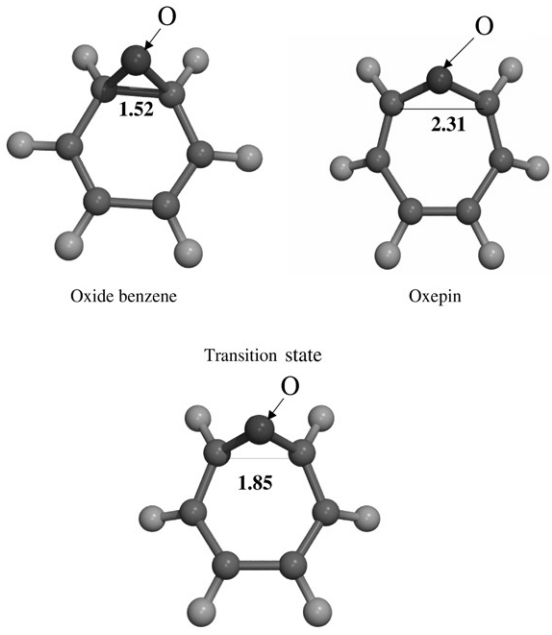

Figure 4. Optimized structures of benzene oxide, oxepin and the transition state of their tautomerization.

Table 1
Changes in total energies during the transformation (in kJ/mol)

Structure	ΔE
Benzene oxide → oxepin	+2.9
Benzene oxide → TS (benzene oxide–oxepin)	+25.9

energy of benzene oxide formation or its absence. Also we performed geometry optimization of benzene oxide and oxepin adsorbed on our OFe/ZSM5 model cluster. Optimized models are shown in figure 5. The structural comparison of the free benzene oxide and oxepin, and ones adsorbed on the cluster show minimum changes in geometries. The bond distances between iron and the reactive oxygen species associated in benzene oxide and oxepin equal 2.03 and 2.07 Å, respectively. Adsorbed benzene oxide is more stable compared to oxepin by 9.5 kJ/mol due to its stronger interaction with Fe. For the free molecules, opposite results were found. The energetic effects of the transformations are presented in table 2. The energy of benzene oxide formation from free benzene and the initial OFe/Z cluster equals −96.0 kJ/mol. The ease of benzene oxide formation during the adsorption of benzene on the oxygen-containing α-center allows the conclusion that step (1) is not rate limiting. The process of phenol formation (2) proceeds via breaking of a C–H bond. The question of the experimental evidence of the absence of the KIE is of interest. It can be explained by the fact that the process consists of a few steps. It is interesting that the reaction of benzene oxide to phenol in solution also showed the absence of the KIE [39]. The stepwise mechanism of the aromatization of arene oxides was suggested in these studies [40]:

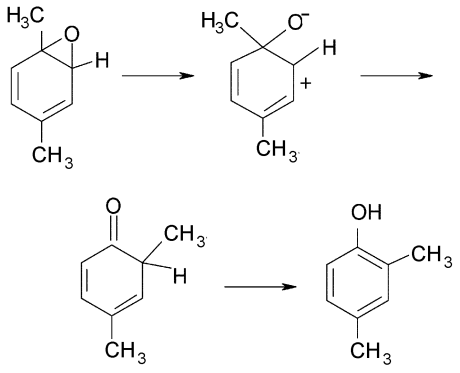

The transfer of the arene oxide to zwitterions has been proposed to be the rate-limiting step, in agreement with the absence of the KIE [39]. It was also shown experimentally that proton acidity catalyzed this process [41]. A theoretical study of elementary channels of the reaction $C_6H_6 + O$ (^3P) [42] also considered the formation of the keto tautomer of phenol and phenol with the biradical structure, which is a direct analog of the zwitterion in the case of the singlet state of the reaction

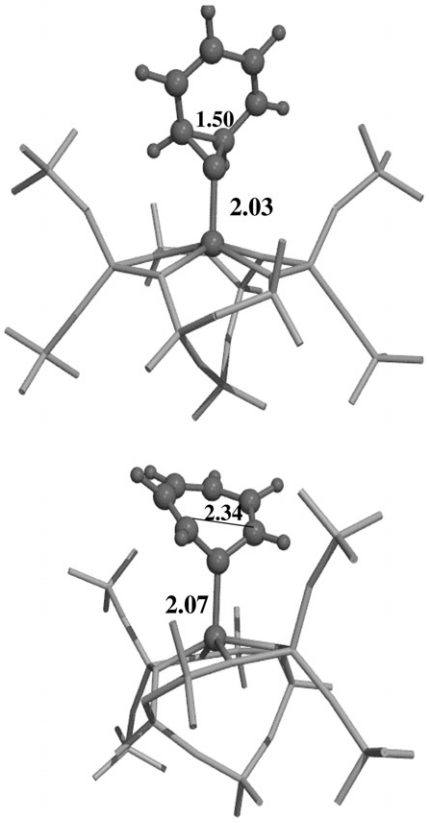

Figure 5. Optimized structures of benzene oxide and oxepin adsorbed on OFe/ZSM-5 model cluster.

system. In both cases this intermediate appeared to be the key one.

In the next step we studied the evolution of benzene oxide by breaking one of the two C–O bonds. The resulting intermediate is shown in figure 6. This intermediate is less stable by 29.0 kJ/mol than adsorbed benzene oxide. According to our calculations, formation of this intermediate is a potential candidate for the rate-limiting step of benzene to phenol conversion. This would also comply with the experimental observation of the absence of the KIE. Although this intermediate was not observed, its formation is mentioned in a number of papers [41,42]. One possible pathway for the transformation of this intermediate is the formation of the keto tautomer of phenol. The idea of keto tautomer formation during photolysis of benzene oxide has been stated in

Table 2
Energetic effects (in kJ/mol) of the transformations compared to the free benzene and OFe/ZSM-5

Structure	ΔE
C_6H_6 (free) + O=Fe/ZSM-5	0.0
Oxepin (ads.) + Fe/ZSM-5	−86.5
Benzene oxide (ads.) + Fe/ZSM-5	−96.0
Intermediate + Fe/ZSM-5	−67.0
Keto tautomer + Fe/ZSM-5	−243.3
Phenol + Fe/ZSM-5	−260.0

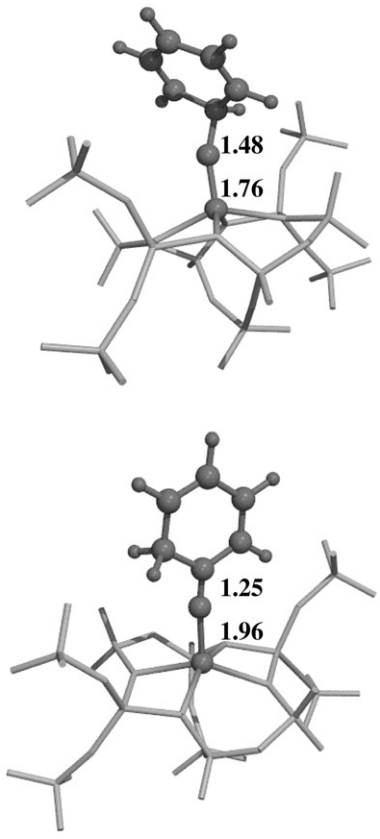

Figure 6. Optimized structures of the intermediate and keto tautomer of phenol.

the literature [43] and is in agreement with our study. The optimized structure of the keto tautomer is shown in figure 6. The transformation of the intermediate to keto tautomer is favorable, about −176.3 kJ/mol. A further indication for the formation of this keto tautomer is found in IR studies during conversion of benzene to phenol [27]. We calculated the IR spectra for free benzene, phenol, benzene oxide, oxepin and the phenol keto tautomer molecules. The vibrational frequencies of these molecules are presented in table 3. The band shift (about 200 cm^{-1}) is found only for the keto tautomer of phenol. Thus, we attribute the experimentally observed band at 2874 cm^{-1} [27] to C–H vibrations of the CH_2 group of the keto tautomer of phenol.

To clarify the reaction path for benzene hydroxylation, the adsorption complex of phenol with Fe/ZSM5 was further studied. Figure 7 shows the optimized structure. The basic structure of the phenol moiety in the product complex is not significantly changed from that of free phenol. The Fe–O distance of 2.11 Å is slightly longer than 2.03 and 2.07 Å in the arene oxide intermediates. The Fe–O bond of the product complex is thus viewed as a typical coordinate bond similar to those of the intermediates. The energy of transformation of benzene oxide to phenol on Fe/ZSM-5 is 164.0 kJ/mol and from keto tautomer to phenol is −16.7 kJ/mol. This value includes the difference in the energies of free

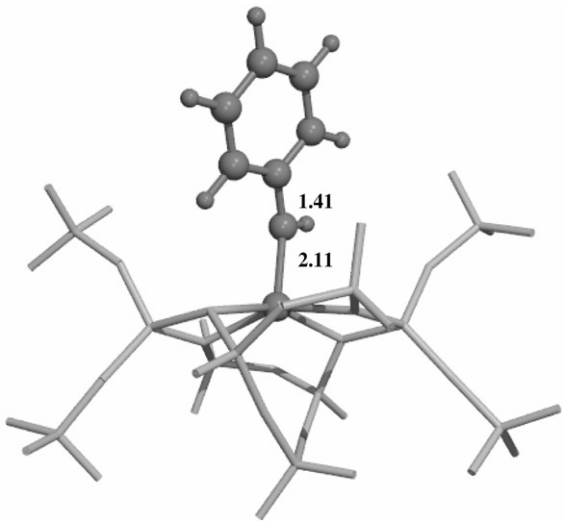

Figure 7. Structure of the adsorption complex of phenol with Fe/ZSM-5.

phenol and benzene oxide or its keto tautomer and the difference in adsorption energies on the zeolite cluster. Data of adsorption energies of the different products on Fe/ZSM-5 are presented in table 4. The adsorption energy of phenol on Fe/ZSM-5 equals −96.1 kJ/mol.

Table 3
C–H vibrational frequencies (cm^{-1}) for free reactant, product and possible intermediates

Structure	Frequency
Keto tautomer	3029 sym. CH_2
	3052 asym. CH_2
	3176
	3181
	3205
	3216
Benzene	3176 b_{1u}
	3185 e_{2g}
	3185 e_{2g}
	3201 e_{1u}
	3201 e_{1u}
	3212 a_{1g}
Phenol	3180
	3187
	3195
	3204
	3212
Oxepin	3162
	3170
	3173
	3185
	3192
Benzene oxide	3163
	3168
	3181
	3190
	3203
	3210

Table 4
Adsorption energies of the different products on Fe/ZSM-5

Structure	Adsorption energy (kJ/mol)
Benzene oxide	−113
Oxepin	−100
Keto tautomer	−134
Phenol	−96

The final complex from which phenol is released involves Fe^{2+} that needs to be regenerated back to Fe–O upon decomposition of N_2O. Summarizing, the calculated data indicate that the reaction path for the hydroxylation of benzene proceeds as follows:

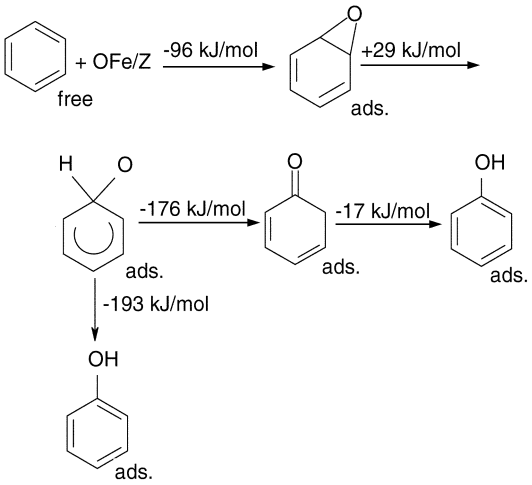

For the total mechanism this implies that the desorption of phenol is the key step in the total reaction process as is confirmed by recent experimental observations [44].

3.3. Intramolecular benzene oxide transformation to the zwitterion intermediate for free molecules and for acidic catalysis

Let us look in detail at the energy of the benzene oxide transformation to the zwitterion intermediate, which is of relevance for the proton-catalyzed reaction in solution. The energetic effects of the transformations are summarized in table 5. The optimized structures of the protonated intermediates are shown in figure 8. The intermediate is less stable than benzene oxide by 90.3 kJ/mol. It is important to note that the calculation

Table 5
Energetic effects of the transformations (in kJ/mol)

Transformation	ΔE
Benzene oxide (HF) → intermediate (CAS SCF)	+90.3
Protonated benzene oxide → protonated intermediate	−62.3

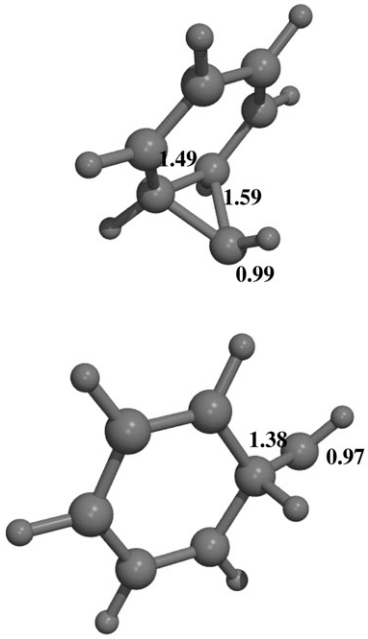

Figure 8. Optimized structures of protonated benzene oxide and intermediate.

of the free zwitterion intermediate can only be done satisfactorily by using the CAS SCF method. For the protonated structures, the intermediate is more stable by 62.3 kJ/mol compared to benzene oxide which agrees with acidic catalytic data for the reaction.

4. Conclusion

DFT cluster model calculations were carried out on a model for the α-oxygen active site present in Fe ions occluded in the micropores of ZSM-5. The model consisted of an Fe(II) ion at the α-cationic position of the MFI structure. The calculated bond energy for α-oxygen agreed well with experiment. We found that its interaction with benzene resulted in facile formation of arene oxide suggesting that this step is not rate limiting. The arene oxide was subsequently transformed into phenol in a stepwise mechanism. All possible intermediates (benzene oxide, oxepin, the zwitterion, the keto tautomer and phenol) were studied in the adsorbed state on the active site. By analogy with the rate-limiting step in solutions, the transformation of arene oxide to the zwitterion was found to be a difficult step. This agrees with the absence of the kinetic H/D isotope effect. The experimentally observed frequency of 2874 cm^{-1} during adsorption of benzene on α-sites of zeolite could be attributed to CH_2 vibrations in the adsorbed keto tautomer of phenol. Adsorbed phenol occurs as the most stable final product and, most probably, phenol desorption by substitution with nitrous oxide is the key step in the total reaction scheme.

Acknowledgments

The Dutch Science Foundation is gratefully acknowledged for the financial support of the collaborative Russian–Dutch Project NWO-19-0411999. The authors also thank S.P. Ruzankin, X. Rozanska, P. Vassilev, A.S. Kharitonov and K.A. Dubkov for helpful discussions.

References

[1] G.I. Panov, V.I. Sobolev and A.S. Kharitonov, J. Molec. Catal. 61 (1990) 85.
[2] G.I. Panov, CATTECH 4 (2000) 18.
[3] G. Berlier, G. Spoto, S. Bordiga, G. Ricchiardi, P. Fisicaro, A. Zecchina, I. Rossetti, E. Selli, L. Forni, E. Giamello and C. Lamberti, J. Catal. 208 (2002) 64.
[4] A.M. Ferretti, C. Oliva, L. Forni, G. Berlier, A. Zecchina and C. Lamberti, J. Catal. 208 (2002) 83.
[5] A.L. Yakovlev and G.M. Zhidomirov, Catal. Lett. 63 (1999) 91.
[6] G.I. Panov, A.S. Kharitonov and V.I. Sobolev, Appl. Catal. A: General 98 (1993) 1.
[7] P.P. Notte, Topics Catal. 13 (2000) 387.
[8] H.Y. Chen, E.M. El-Malki, X. Wang, R.A. van Santen and W.M.H. Sachtler, J. Mol. Catal. A: Chem. 162 (2000) 159.
[9] K.A. Dubkov, N.S. Ovanesyan, A.A. Shteinman, E.V. Starokon and G.I. Panov, J. Catal. 207 (2002) 341.
[10] J. Perez-Ramirez, F. Kapteijn, G. Mul and J.A. Moulijn, Catal. Commun. 3 (2002) 19.
[11] A.S. Kharitonov, G.I. Panov, G.A. Sheveleva, L.V. Pirutko, T.P. Voskresenskaya and V.I. Sobolev, Russian Patent 2074164.
[12] S. Bordiga, R. Buzzoni, F. Geobaldo, C. Lamberti, E. Giamello, A. Zecchina, G. Leofanti, G. Petrini, G. Tozzola and G. Vlaic, J. Catal. 158 (1996) 486.
[13] El-M. El-Malki, R.A. van Santen and W.M.H. Sachtler, J. Catal. 196 (2000) 212.
[14] H.-Y. Chen, T.V. Voskoboinikov and W.M.H. Sachtler, J. Catal. 180 (1998) 171.
[15] H.-Y. Chen and W.M.H. Sachtler, Catal. Today 42 (1998) 73.
[16] P. Marturano, L. Drozdova, A. Kogelbauer and R. Prins, J. Catal. 192 (2000) 236.
[17] A.A. Battiston, J.H. Bitter and D.C. Koningsberger, Catal. Lett. 66 (2000) 75.
[18] A.L. Yakovlev, G.M. Zhidomirov and R.A. van Santen, J. Phys. Chem. B 105 (2001) 12297.
[19] (a) Q. Zhu, B.L. Mojet, R.A.J. Janssen, E.J.M. Hensen, J. van Grondelle, P.C.M.M. Magusin and R.A. van Santen, Catal. Lett. 81 (2002) 205; (b) Q. Zhu, E.J.M. Hensen, B.L. Mojet, J.H.M.C. van Wolput and R.A. van Santen, Chem. Commun. (2002) 1232.
[20] N.S. Ovanesyan, A.A. Shteinman, V.I. Sobolev, K.A. Dubkov and G.I. Panov, Kinetica I Kataliz, 39 (1998) 863.
[21] J. Perez-Ramirez, G. Mul, F. Kapteijn, J.A. Moulijn, A.R. Overveg, A. Domenech, A. Ribera and I.W.C.E. Arends, J. Catal. 207 (2002) 113.
[22] B. Wichterlová, J. Dědeček and Z. Sobalík, in: *12th International Zeolite Conference* (Materials Research Society, 1999) p. 941.
[23] M.J. Rice, A.K. Chakraborty and A.T. Bell, J. Phys. Chem. B 104 (2000) 9987.
[24] A.A. Shubin, G.M. Zhidomirov, A.L. Yakovlev and R.F. van Santen, J. Phys. Chem. B 105 (2001) 4928.
[25] G.I. Panov, A.K Uriarte, M.A. Rodkin and V.I. Sobolev, Catal. Today 41 (1998) 365.
[26] K.A. Dubkov, V.I. Sobolev, E.P. Talsi, N.H. Watkins, A.A. Shteinman and G.I. Panov, J. Molec. Catal. 123 (1997) 155.
[27] G.I. Panov, K.A. Dubkov and Y.A. Paukshtis, in: *Catalysis by Unique Metal Ion Structures in Solid Matrices*, eds. G. Centi, B. Wichterlová and A.T. Bell, Vol. 13 (Kluwer Academic, Dordrecht, Boston, London, 2001) p. 149.
[28] K. Yoshizava, Y. Shiota, T. Yumura and T. Yamabe, J. Phys. Chem. B 104 (2000) 734.
[29] A.D. Becke, Phys. Rev. A 38 (1988) 3098; J. Chem. Phys. 98 (1993) 1372; J. Chem. Phys. 98 (1993) 5648.
[30] S.K. Loh, E.R. Fisher, L. Lian, R.H. Schultz and P. B Armentrout, J. Phys. Chem. 93 (1989) 2601.
[31] M.N. Glukhovtsev, R.D. Bach and C.J. Nagel, J. Phys. Chem. A 101 (1997) 316.
[32] D. Hegarty and M.A. Robb, Mol. Phys. 38 (1979) 1795.
[33] R.H.E. Eade and M.A. Robb, Chem. Phys. Lett. 83 (1981) 362.
[34] D.M. Jerina and J.W. Daly, Science 185 (1974) 573.
[35] B. Klotz, I. Barnes, K.H. Becker and B.T. Golding, J. Chem. Soc. Faraday Trans. 93 (1997) 1507.
[36] C.C. Pye, J.D. Xidos, R.A. Poirier and D.J. Burnell, J. Phys. Chem. A 101 (1997) 3371.
[37] E. Vogel, W.A. Böll and H. Günther, Tetrahedron Lett. (1965) 609.
[38] E. Vogel and H. Günther, Angew. Chem., Int. Ed. Engl. 6 (1967) 385.
[39] G.J. Kasperek, P.Y. Bruce, T.C. Bruce, H. Yagi and D.M. Jerina, J. Chem. Soc. Commun. (1972) 784.
[40] G.J. Kasperek, T.C. Bruce, H. Yagi and D.M. Jerina, J. Am. Chem. Soc. 95 (1973) 6041.
[41] G.J. Kasperek and T.C. Bruce, J. Am. Chem. Soc. 94 (1972) 152.
[42] D. Hudson, H.-Y. Zhang, M.R. Nimlos and J.T. McKinnon, J. Phys. Chem. A 105 (2001) 4316.
[43] D.M. Jerina, B. Witkop, C.L. McIntosh and O.L. Chapman, J. Am. Chem. Soc. 96 (1974) 5578.
[44] A.A. Ivanov, V.S. Chernavsky, A.S. Kharitonov and G.I. Panov, Appl. Catal. (submitted).